Letter

Polarons and their induced interactions in highly imbalanced triple mixtures

Kevin Keiler,[1] Simeon I. Mistakidis,[1] and Peter Schmelcher[1,2]
[1]*Center for Optical Quantum Technologies, Department of Physics, University of Hamburg, Luruper Chaussee 149, 22761 Hamburg, Germany*
[2]*Hamburg Centre for Ultrafast Imaging, University of Hamburg, Luruper Chaussee 149, 22761 Hamburg, Germany*

(Received 8 December 2020; revised 23 July 2021; accepted 24 August 2021; published 7 September 2021)

We unravel the polaronic properties of impurities immersed in a correlated trapped one-dimensional Bose-Bose mixture. This setup allows the impurities to couple either attractively or repulsively to a specific host, thus offering a highly flexible platform for steering the emergent polaronic properties. Specifically, the impurity residue peak and strength of induced interactions can be controlled by varying the coupling of the impurities to the individual bosonic components. In particular, it is possible to maintain the quasiparticle character for larger interaction strengths as compared to the case of impurities immersed in a single bosonic species. We explicate a hierarchy of the polaron binding energies in terms of the impurity-medium interactions, thereby elucidating the identification of the polaronic resonances in recent experimental radio-frequency schemes. For strong attractive impurity-medium couplings, bipolaron formation is captured. Our findings pave the way for continuously changing the quasiparticle character, under the impact of trap effects, while exposing the role of correlations in triple-mixture settings.

DOI: 10.1103/PhysRevA.104.L031301

I. INTRODUCTION

Ultracold atoms provide pristine platforms for probing quantum phenomena in multicomponent fermionic and bosonic [1,2] settings offering an exquisite tunability [1,3,4]. Highly-particle-imbalanced mixtures [5–8] have recently received major attention in terms of the quasiparticle context [9], leading to fundamentally new insights concerning Fermi and Bose polarons [5,10,11] and thus serving as a quantum simulator of the corresponding condensed-matter setup. The quasiparticle notion extends far beyond cold-atom settings in semiconducting [12] and superconducting devices [13], while interactions among quasiparticles in liquid-helium mixtures [14,15] and cuprates [16,17] are a promising candidate for conventional and high-T_c superconductivity [18–24]. Owing to the recent experimental realization of these impurity systems [6–8,25–30], intense theoretical activity has been triggered for the investigation of their stationary properties [31,32], e.g., unveiling their effective mass [33–35], excitation spectra [7,11,36,37], and induced interactions [38–48]. Only very recently have extensions to impurities interacting with a coherently coupled two-component Bose-Einstein condensate (BEC) [49,50] and Bose-Bose mixtures [51] been considered, while introducing holes in spinor fermionic lattice setups has led to the concept of magnetic polarons [52–54]. The description of such systems is expected to necessitate higher-order correlations [55–59], thus invalidating lower-order approaches [51,60–74], as already demonstrated in binary systems.

The generalization to triple-mixture settings allows for the impurities to selectively couple to the individual hosts, thus offering an efficient platform for tuning the emergent polaronic properties. This includes the longevity, i.e., the prevention of orthogonality catastrophe, the mobility of the polarons, and the control of their induced interactions. Additionally, it enables the design of their magnetic and spin-mixing processes by the use of Raman coupling and the design of intriguing bound states such as dimers and trimers as shown for an impurity in a double Fermi sea [75]. Being experimentally within reach of current state-of-the-art experiments [76,77], triple mixtures will exhibit more complex quantum phases as compared to their binary counterpart. In this sense, the possibility for the cumulative bath to be prepared in the well-known corresponding phases of a binary mixture, such as in any combination of Tonks-Girardeau gases, a miscible phase, and an immiscible phase [78], will naturally impact the quasiparticle character. This will shed light on the polaron problem from a very different perspective as the impurities are dressed by the excitations of two different hosts. Utilizing an *ab initio* approach, as we do here, it is possible to enter unexplored regimes where correlations are dominant, thereby serving in particular as a benchmark for future experimental implementations of triple-mixture setups as well as effective theoretical models.

For these reasons, in this Letter we undertake an initial step in this direction and explore the polaronic properties of impurities coupled to a one-dimensional [4,79] harmonically trapped Bose-Bose mixture spanning a wide range of attractive and repulsive impurity-medium coupling strengths while including all particle correlations. Commonly polarons are studied in spatially uniform systems, while we account for trap effects which are relevant to typical ultracold-atom experiments. We exemplify that for a single impurity, the distribution of the impurity residue in terms of the

impurity-medium couplings can be steered by adjusting the different interactions to the respective baths of the mixture. In particular, when coupling repulsively to one host and attractively to the other one, the residue peak can be broadened such that the polaronic character is maintained for larger interaction strengths. For strong repulsive or attractive impurity-medium interactions, the impurity residue vanishes. The behavior of the dressed impurity can be intuitively interpreted in terms of an effective potential, which provides a good approximation for weak impurity-bath coupling strengths, where interspecies entanglement is suppressed. The location of the attractive and repulsive quasiparticle resonances is captured by monitoring the polaron binding energy. Upon considering two bosonic impurities, we identify the presence of attractive induced interactions whose strength can be steered by the coupling to the respective hosts of the Bose-Bose mixture. Induced interactions strongly influence the impurities' spatial distribution allowing, for instance, bipolaron formation and lead to a reduction of the impurity residue.

II. MODEL

We consider a Bose-Bose mixture consisting of two species A and B with equal masses $m_A = m_B = m$ and $N_A = N_B = 10$ particles. We note that our results persist for larger N_A and N_B (see [80–96]). Here $N_C = 1, 2$ bosonic impurities of mass m_C are immersed in this one-dimensional harmonically confined [97,98] mixture of interacting atoms. The trap frequencies are $\omega_A = \omega_B = \omega_C = \omega = 1.0$. The many-body (MB) Hamiltonian of the system reads

$$\hat{H} = \sum_{\sigma\in\{A,B,C\}} \hat{H}_\sigma + \hat{H}_{AB} + \hat{H}_{AC} + \hat{H}_{BC}. \tag{1}$$

Here $\hat{H}_\sigma = \int dx\, \hat{\Psi}^\dagger_\sigma(x)(-\frac{\hbar^2}{2m_\sigma}\frac{d^2}{dx^2} + \frac{1}{2}m_\sigma\omega_\sigma^2 x^2)\hat{\Psi}_\sigma(x) + g_{\sigma\sigma}\int dx\, \hat{\Psi}^\dagger_\sigma(x)\hat{\Psi}^\dagger_\sigma(x)\hat{\Psi}_\sigma(x)\hat{\Psi}_\sigma(x)$ describes the Hamiltonian of species $\sigma \in \{A, B, C\}$, with contact intraspecies interaction of $g_{AA} = g_{BB} > 0$ and $g_{CC} = 0$. In addition, $\hat{\Psi}_\sigma(x)$ is the σ-species bosonic field operator. Further, $\hat{H}_{\sigma\sigma'} = g_{\sigma\sigma'}\int dx\, \hat{\Psi}^\dagger_\sigma(x)\hat{\Psi}_\sigma(x)\hat{\Psi}^\dagger_{\sigma'}(x)\hat{\Psi}_{\sigma'}(x)$ defines the contact interspecies interaction of strength $g_{\sigma\sigma'}$ [99]. In this sense, $\hat{H}_A + \hat{H}_B + \hat{H}_{AB}$ build the Bose-Bose mixture serving as a cumulative bath for the impurity species, described by $\hat{H}_C$. The impurities couple repulsively or attractively to both A and B hosts via a contact interaction of strengths g_{AC} and g_{BC}, as captured by $\hat{H}_{AC}$ and $\hat{H}_{BC}$. To directly expose the pure effect of impurity-impurity induced interactions we set $g_{CC} = 0$. We focus on the case of equal masses $m = m_C$, which can be experimentally realized to a good approximation by considering a mixture of isotopes, e.g., a ^{87}Rb BEC where the Bose-Bose mixture refers to two hyperfine states [100,101] and ^{85}Rb for the impurities. The effects of mass imbalance are discussed in Ref. [80]. Throughout this work, we consider $g_{AA} = g_{BB} = 0.2$ and $g_{AB} = 0.1$ in units of $\sqrt{\hbar^3\omega/m}$, leading to a miscible mixture of species A and B. Spatial scales are given in harmonic units of $\sqrt{\hbar/m\omega}$ and energies in terms of $\hbar\omega$. To address the ground state of our three-component system we use the variational multilayer multiconfiguration time-dependent Hartree method for atomic mixtures (MLMCTDHX) [102–104]. This nonperturbative approach relies on expanding the MB wave function with respect to a variationally optimized time-dependent basis [80].

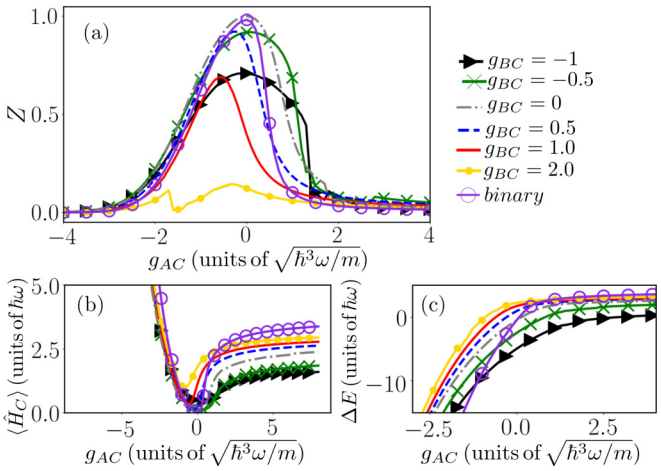

FIG. 1. (a) Impurity residue Z, (b) polaron energy $\langle\hat{H}_C\rangle$, and (c) polaron binding energy ΔE for different impurity-bath couplings g_{AC} and g_{BC}. The violet circles represent the binary mixture with $N = 20$ single-species bath atoms and $g = 0.2$.

III. RESULTS AND DISCUSSION

As a first step, we vary the individual impurity-medium coupling strengths g_{AC} and g_{BC} of a single impurity to the cumulative bath from attractive to repulsive values and obtain the ground state of the triple mixture. The underlying impurity residue Z [5] is determined by

$$Z = |\langle\Psi_0|\Psi\rangle|^2, \tag{2}$$

where $|\Psi_0\rangle$ is the MB wave function for a noninteracting impurity with $g_{AC} = g_{BC} = 0$, while $|\Psi\rangle$ denotes the interacting case. Additionally, we determine the impurity residue for a binary mixture, which we define here as an impurity immersed into a bath of $N = 20$ single-species bosons interacting repulsively with a strength of $g = 0.2$. Figure 1(a) illustrates the impurity residue upon varying the impurity-bath couplings g_{AC} and g_{BC}. In all cases we find that Z exhibits a broad peak around $Z = 1$ with respect to g_{AC} and decreases for finite positive and negative g_{AC}, implying the dressing of the impurity and thus its emergent polaronic character [74]. The reduction of Z towards zero for strong repulsions g_{AC} and g_{BC} is caused by the phase separation of the impurity with its hosts,[1] thus rendering no dressing possible (see [80]). In contrast, for strong attractions $g_{AC} \ll 0$ the impurity either lies within both hosts for $g_{BC} < 0$ or solely resides within host A while host B forms a shell structure for $g_{BC} > 0$ [80]. In the latter case the density of host B localizes towards the trap edges, thereby encapsulating the other two species which reside around the trap center forming the core. As a result of the strong binding

[1]For large g_{AC} and $g_{BC} < 0$, host A (core) phase separates with the impurity (shell), while host B forms a less pronounced shell structure, leading to a minor dressing of the impurity.

of the impurity with at least one of the baths and the potential phase separation with the species B, the impurity residue decreases towards zero. The width of the residue distribution for $g_{BC} = 0$ is larger than for the binary system due to the smaller interspecies coupling strength $g_{AB} = 0.1$, as compared to the intraspecies interaction $g = 0.2$. For repulsive g_{BC} we observe a decrease and shift of the impurity residue peak with increasing g_{BC} as compared to the case of $g_{BC} = 0$ and the binary mixture. These phenomena are again attributed to the presence of the impurity-host phase separation taking place for a larger range of values of g_{AC} with increasing g_{BC} (see Ref. [80]). Furthermore, the width of the residue distribution decreases for increasingly repulsive values of g_{BC}. Note the sudden decrease and subsequent increase of Z for $g_{BC} = 2.0$ and attractive $g_{AC} \simeq -1.8$, which is an imprint of a weak phase separation of the impurity and the host A with species B (see Ref. [80]). However, for attractive g_{BC} a broadening of the residue distribution occurs towards repulsive values of the couplings g_{AC}, as well as the corresponding value of the maximum. The fact that $Z < 1$ for $g_{AC} = 0$ is attributed to the finite coupling g_{BC}, leading already to polaron formation by the host B, while for $g_{AC} \neq 0$ the polaron experiences an additional dressing. Importantly, a powerful asset of the binary host is that, depending on the combination of attractive and repulsive impurity-bath couplings, it is possible to flexibly control and maintain the polaron for larger values of the coupling strength g_{AC} to the medium. This effect can also be retrieved for heavier impurities, e.g., with mass ratios $m/m_C = 87/133$ and $m/m_C = 87/174$, where the baths consist of ^{87}Rb atoms and the impurities are either ^{133}Cs or ^{174}Yb atoms, respectively (see Ref. [80]).

The competition of the impurity-medium coupling strengths also naturally impacts the polaronic energy $\langle \hat{H}_C \rangle = \langle \Psi | \hat{H}_C | \Psi \rangle - \langle \Psi_0 | \hat{H}_C | \Psi_0 \rangle$ [Fig. 1(b)]. While for increasingly attractive g_{AC} an increase of the energy occurs for arbitrary values of g_{BC}, for repulsive g_{AC} the energy tends to saturate towards different values depending on g_{BC} (discussed below). For $g_{BC} > 0$ and $g_{AC} > 0$ we generally encounter larger polaron energies, suggesting an increasing effective mass [74] as compared to the case $g_{BC} < 0$. Consequently, it is possible to distinguish between repulsive and attractive impurity-bath coupling strengths g_{BC} based on the corresponding polaron energy. Next we estimate the polaron binding energy

$$\Delta E = E(N_C, g_{AC}, g_{BC}) - E(N_C = 0, g_{AC} = 0, g_{BC} = 0) \quad (3)$$

being defined as the energy difference due to the injection of the impurity, where $E(N_C, g_{AC}, g_{BC})$ is the total energy of the system with N_C impurities interacting with an effective strength g_{AC} and g_{BC} with the respective species [Fig. 1(c)]. As expected, ΔE decreases for increasingly attractive g_{AC} and saturates for repulsive values, similarly to the behavior of $\langle \hat{H}_C \rangle$. The former can be associated with a strong binding of the impurity to its hosts, thereby reducing ΔE, while the latter is a consequence of the resultant phase-separation process where the impurity forms a shell structure around the baths [80]. Evidently, we find a clear hierarchy of ΔE depending on g_{BC}, namely, decreasing g_{BC} apparently leads to a reduction of ΔE for any fixed g_{AC}. Therefore, experimentally, e.g., utilizing a radio-frequency scheme [105,106], the corresponding polaronic resonances are clearly distinguishable from

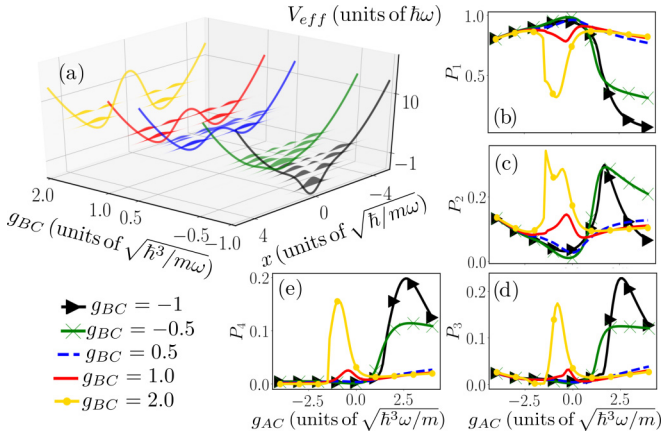

FIG. 2. (a) Effective potential V_{eff} and corresponding eigenvector distributions $|\phi_i(x)|^2$ for $g_{AC} = 0.5$ and different g_{BC}. (b)–(e) Probability of finding the impurity in the single-particle eigenstate $|\phi_i\rangle$, $i = 1, 2, 3, 4$, of V_{eff}.

each other. We have verified that a similar behavior of ΔE takes place for a larger cumulative bath with $N_A = N_B = 50$ particles [80].

To offer an intuitive understanding into the impurity's state for varying g_{AC} and g_{BC}, we construct an effective potential [107] by considering the Bose-Bose mixture as a static potential superimposed to the harmonic confinement of the impurity. It reads

$$V_{\text{eff}} = \tfrac{1}{2} m_C \omega^2 x^2 + g_{AC} \rho_A^{(1)}(x) + g_{BC} \rho_B^{(1)}(x), \quad (4)$$

where $\rho_\sigma^{(1)}(x)$ is the one-body density of $\sigma = A, B$ bath species calculated within the correlated MB approach and thereby includes all necessary correlations. Accordingly, the impurity may occupy the eigenstates $|\phi_i\rangle$ of V_{eff}; V_{eff} neglects several phenomena such as the renormalization of the impurity's mass as well as the possible emergence of induced interactions. Figure 2(a) shows the deformations of the effective potential and its underlying eigenstates $|\phi_i\rangle$ under variations of g_{BC} for $g_{AC} = 0.5$. For $g_{BC} \ll 0$, specifically, $g_{BC} = -1$, the harmonic-oscillator potential exhibits an additional dip which becomes more prominent with decreasing g_{BC}, whereas for $g_{BC} > 0$ a double-well structure forms. This has an impact on the related eigenstates such that quasidegeneracies develop. The probability of finding the impurity in the ith eigenstate of V_{eff} irrespectively of the states that are populated by the Bose-Bose mixture is given by

$$P_i = \sum_{kl} |\langle \vec{n}_k^A | \langle \vec{n}_l^B | \langle \phi_i | \Psi \rangle|^2, \quad (5)$$

where $\{|\vec{n}^\sigma\rangle\}$ is an arbitrary complete Fock basis of the $\sigma = A, B$ baths. For all g_{BC}, except for $g_{BC} = 2.0$, the ground state of the impurity is well described, i.e., $P_1 > 0.9$, by the corresponding ground state within the effective potential for weak attractive and weak repulsive g_{AC} [Fig. 2(b)]. Further decreasing g_{AC} towards attractive couplings, the occupation of $|\phi_1\rangle$ is reduced, whereas $|\phi_2\rangle$ starts to contribute [Fig. 2(c)]. This behavior can still be recovered for $g_{AC} > 0$, while for attractive impurity-bath couplings $g_{BC} < 0$ and $g_{AC} > 0$ we find a drastic decrease of P_1 accompanied by the substantial

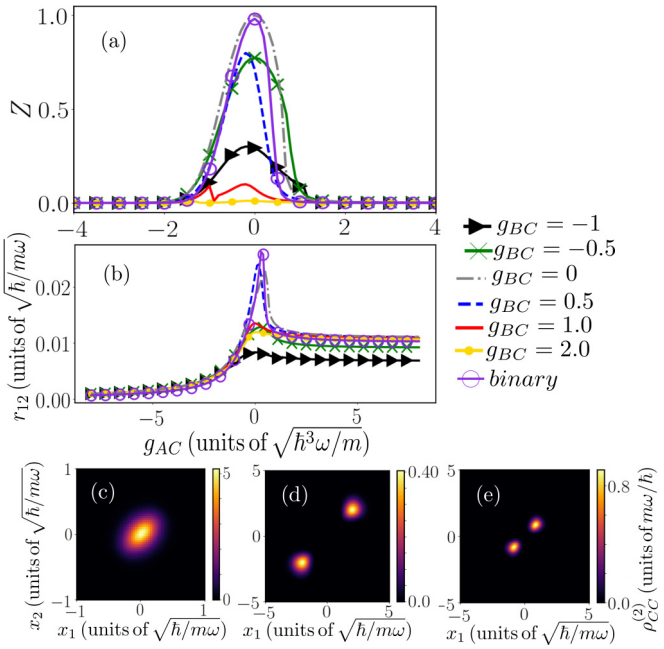

FIG. 3. (a) Two-impurity residue Z and (b) distance r_{12} for $N_C = 2$ upon varying the impurity-bath couplings g_{AC} and g_{BC}, while $g_{CC} = 0$. The violet circles represent the binary mixture with $N = 20$ bath atoms. Also shown is the two-body density $\rho^{(2)}_{CC}(x_1, x_2)$ of the two impurities for combinations (g_{AC}, g_{BC}) of (c) $(-2.1, -1)$, (d) (8,2), and (e) $(8, -1)$.

occupation of the excited states $|\phi_2\rangle$, $|\phi_3\rangle$, and $|\phi_4\rangle$ [Figs. 2(c)–2(e)]. Accordingly, the effective potential picture is no longer valid and does not provide a proper description of the impurity coupled to a cumulative bath. This is in line with the behavior of the impurity residue Z, which drops to zero in this interaction range [Fig. 1(a)].

Let us now discuss the behavior of $N_C = 2$ bosonic impurities immersed in a Bose-Bose mixture. Monitoring the two-impurity residue [Eq. (2)] in order to extract the impact of the coupling on the impurities, we generally observe behavior [Fig. 3(a)] similar to that for the single-impurity case. For $g_{BC} < 0$ the peaks of Z are broadened while being reduced in height, whereas for $g_{BC} > 0$ a smaller width of the residue distribution is encountered compared to $N_C = 1$. The effect of the additional impurity can be evinced in the strong suppression of the peak height of Z for all finite impurity-bath couplings g_{BC} (e.g., a reduction by approximately 50% for $g_{BC} = -1$), signaling stronger coherence losses when compared to the $N_C = 1$ scenario [106]. Consequently, this leads to a decreasing two-impurity residue Z. In the case of $N_C = 2$ the question regarding their effective interactions mediated by the hosts and being naturally related to their relative distance arises. This cannot be inferred from Z. For this reason we analyze the experimentally tractable [108] impurity distance [40,47,109]

$$r_{12} = \iint dx_1 dx_2 |x_1 - x_2| \rho^{(2)}_{CC}(x_1, x_2), \tag{6}$$

with $\rho^{(2)}_{CC}(x_1, x_2) = \langle \Psi | \hat{\Psi}^\dagger_C(x_1) \hat{\Psi}^\dagger_C(x_2) \hat{\Psi}_C(x_1) \hat{\Psi}_C(x_2) | \Psi \rangle$ the two-body density of two impurities providing the probability of finding simultaneously one impurity at position x_1 and the other one at x_2. Around $g_{AC} = 0$ we find a peak of the impurities' distance, which is most pronounced for $g_{BC} = 0$, $g_{BC} = 0.5$, and the binary system [Fig. 3(b)]. In all cases the manifestation of attractive induced interactions mediated by the hosts is evident by the decreasing behavior of r_{12} for finite g_{AC}. Accordingly, the strength of the induced interactions in the region of the existence of the polaron becomes stronger when considering two hosts. More precisely, r_{12} features a decreasing trend towards zero for $g_{AC} < 0$, while for $g_{AC} > 0$ it saturates to a finite value. These finite values of r_{12} barely differ from each other for $g_{BC} \geqslant 0$ and in the case of the binary system. In sharp contrast, for $g_{BC} < 0$ a saturation towards smaller distances is observed, indicating that the impurities lie closer to one another.

In order to clarify whether indeed induced interactions are established, we further investigate the impurities' two-body spatial distribution. For triple-mixture settings the structure and strength of the induced interactions are completely unexplored. Let us first discuss the interaction regime in which r_{12} is independent of $g_{AC} < 0$ [Fig. 3(b)]. As a characteristic example we present $\rho^{(2)}_{CC}$ for $g_{AC} = -2.1$ and $g_{BC} = -1$ [Fig. 3(c)]. Here the two impurities lie together at the trap center and the probability to be located at different positions is reduced, yielding an elongated pattern along $x_1 = x_2$. Hence, the impurities experience an induced interaction due to the cumulative bath. Importantly, this shrinking along the antidiagonal of $\rho^{(2)}_{CC}$ is indicative of a bound state having formed between the impurities known as a bipolaron state [45–47]. We remark that a bound bipolaron can only be formed for sufficiently attractive g_{AC} in the case of $g_{BC} \geqslant 0$ since the impurities' binding energy is not negative otherwise (not shown). However, for $g_{BC} < 0$ the range of existence for a bound bipolaron extends towards weak repulsive couplings g_{AC}, e.g., around $g_{AC} \approx 1$ for $g_{BC} = -1$. Turning now to the case of $g_{AC} > 0$ for $g_{BC} = 2$ [Fig. 3(d)] it is possible to infer that the impurities form a shell structure, indicating a phase separation with their hosts. Moreover, they tend to occupy the same position, residing in a particular side of the appearing shell [44]. A slight elongation as for $g_{BC} = -1$ and $g_{AC} = -2.1$ [Fig. 3(c)] is also visible. Apart from forming a smaller shell structure for $g_{BC} = -1$ and $g_{AC} = 8$ [Fig. 3(e)], the off-diagonal contribution is suppressed as compared to $g_{BC} = 2$ and $g_{AC} = 8$ [Fig. 3(d)], indicating the enhancement of the impurities induced interactions. This explains the saturation of r_{12} towards a smaller value as compared to $g_{BC} = 2$ [Fig. 3(b)]. In this sense, it is possible to steer the strength of the induced interactions by varying g_{BC} as well as the width of the shell structure formed by the impurities.

IV. CONCLUSION

Our results pave the way for controlling the quasiparticle character and induced interactions as well as exposing the role of correlations in triple-mixture settings. The latter lays the foundation for studying related quantum phase transitions and pattern formation. Considering two impurity species trapped in a lattice and immersed in a medium, repulsively bound bipolarons of two species might be realized [48,110].

Another intriguing step would be to consider the sudden injection of the impurity species [107] into the Bose-Bose mixture for the simulation of experimental spectroscopic techniques [70,105,106] in order to unravel the polaron dynamics. The corresponding spectral response provides characteristic information about the impurity residue and emergent dressed excited states, thus also offering a direct realization of our findings [25,36].

ACKNOWLEDGMENTS

The authors thank C. Weitenberg for detailed feedback on the manuscript. K. K. gratefully acknowledges financial support through a scholarship from the Studienstiftung des Deutschen Volkes. S. I. M gratefully acknowledges financial support through the Lenz-Ising Award of the University of Hamburg.

[1] S. Inouye, J. Goldwin, M. L. Olsen, C. Ticknor, J. L. Bohn, and D. S. Jin, Phys. Rev. Lett. **93**, 183201 (2004).

[2] T. Fukuhara, S. Sugawa, Y. Takasu, and Y. Takahashi, Phys. Rev. A **79**, 021601(R) (2009).

[3] C. Chin, R. Grimm, P. Julienne, and E. Tiesinga, Rev. Mod. Phys. **82**, 1225 (2010).

[4] A. N. Wenz, G. Zürn, S. Murmann, I. Brouzos, T. Lompe, and S. Jochim, Science **342**, 457 (2013).

[5] P. Massignan, M. Zaccanti, and G. M. Bruun, Rep. Prog. Phys. **77**, 034401 (2014).

[6] C. Kohstall, M. Zaccanti, M. Jag, A. Trenkwalder, P. Massignan, G. M. Bruun, F. Schreck, and R. Grimm, Nature (London) **485**, 615 (2012).

[7] M. Koschorreck, D. Pertot, E. Vogt, B. Fröhlich, M. Feld, and M. Köhl, Nature (London) **485**, 619 (2012).

[8] F. Scazza, G. Valtolina, P. Massignan, A. Recati, A. Amico, A. Burchianti, C. Fort, M. Inguscio, M. Zaccanti, and G. Roati, Phys. Rev. Lett. **118**, 083602 (2017).

[9] L. D. Landau, Phys. Z. Sowjetunion **3**, 644 (1933).

[10] F. Grusdt and E. Demler, in *Quantum Matter at Ultralow Temperatures*, Proceedings of the International School of Physics "Enrico Fermi," Course CXCI, Varenna, 2014, edited by M. Inguscio, W. Ketterle, S. Stringari, and G. Roati (IOS, Amsterdam, 2016), p. 325.

[11] R. Schmidt, M. Knap, D. A. Ivanov, J. S. You, M. Cetina, and E. Demler, Rep. Prog. Phys. **81**, 024401 (2018).

[12] M. E. Gershenson, V. Podzorov, and A. F. Morpurgo, Rev. Mod. Phys. **78**, 973 (2006).

[13] *Superconducting Devices*, edited by S. T. Ruggiero, and D. A. Rudman (Academic, Boston, 1990).

[14] J. Bardeen, G. Baym, and D. Pines, Phys. Rev. **156**, 207 (1967).

[15] G. Baym, and C. Pethick, *Landau Fermi-Liquid Theory: Concepts and Applications* (Wiley-VCH, Weinheim, 1991).

[16] D. J. Scalapino, Phys. Rep. **250**, 329 (1995).

[17] J. Sous, M. Chakraborty, R. V. Krems, and M. Berciu, Phys. Rev. Lett. **121**, 247001 (2018).

[18] L. N. Cooper, Phys. Rev. **104**, 1189 (1956).

[19] J. R. Schrieffer, *Theory of Superconductivity* (Avalon, New York, 1983).

[20] A. S. Alexandrov and A. B. Krebs, Sov. Phys. Usp. **35**, 345 (1992).

[21] N. F. Mott, J. Phys.: Condens. Matter **5**, 3487 (1993).

[22] A. S. Alexandrov and N. F. Mott, Rep. Prog. Phys. **57**, 1197 (1994).

[23] E. K. Salje, A. S. Alexandrov, and W. Y. Liang, *Polarons and Bipolarons in High-T_c Superconductors and Related Materials* (Cambridge University Press, Cambridge, 2005).

[24] M. Berciu, I. Elfimov, and G. A. Sawatzky, Phys. Rev. B **79**, 214507 (2009).

[25] J. Catani, G. Lamporesi, D. Naik, M. Gring, M. Inguscio, F. Minardi, A. Kantian, and T. Giamarchi, Phys. Rev. A **85**, 023623 (2012).

[26] T. Fukuhara, A. Kantian, M. Endres, M. Cheneau, P. Schaußß, S. Hild, D. Bellem, U. Schollwöck, T. Giamarchi, C. Gross, I. Bloch, and S. Kuhr, Nat. Phys. **9**, 235 (2013).

[27] N. B. Jørgensen, L. Wacker, K. T. Skalmstang, M. M. Parish, J. Levinsen, R. S. Christensen, G. M. Bruun, and J. J. Arlt, Phys. Rev. Lett. **117**, 055302 (2016).

[28] M.-G. Hu, M. J. Van de Graaff, D. Kedar, J. P. Corson, E. A. Cornell, and D. S. Jin, Phys. Rev. Lett. **117**, 055301 (2016).

[29] Z. Z. Yan, Y. Ni, C. Robens, and M. W. Zwierlein, Science **368**, 190 (2020).

[30] M. G. Skou, T. G. Skov, N. B. Jørgensen, K. K. Nielsen, A. Camacho-Guardian, T. Pohl, G. M. Bruun, and J. J. Arlt, Nat. Phys **17**, 731 (2021).

[31] A. G. Volosniev and H.-W. Hammer, Phys. Rev. A **96**, 031601(R) (2017).

[32] K. Sacha and E. Timmermans, Phys. Rev. A **73**, 063604 (2006)

[33] F. Grusdt, G. E. Astrakharchik, and E. A. Demler, New J. Phys. **19**, 103035 (2017).

[34] D. C. Khandekar, K. V. Bhagwat, and S. V. Lawande, Phys. Rev. B **37**, 3085 (1988).

[35] L. A. Peña Ardila and S. Giorgini, Phys. Rev. A **92**, 033612 (2015).

[36] M. Cetina, M. Jag, R. S. Lous, I. Fritsche, J. T. Walraven, R. Grimm, J. Levinsen, M. M. Parish, R. Schmidt, M. Knap, and E. Demler, Science **354**, 96 (2016).

[37] H. Tajima and S. Uchino, Phys. Rev. A **99**, 063606 (2019).

[38] C. Charalambous, M. A. Garcia-March, A. Lampo, M. Mehboud, and M. Lewenstein, SciPost Phys. **6**, 010 (2019).

[39] P. Naidon, J. Phys. Soc. Jpn. **87**, 043002 (2018).

[40] S. I. Mistakidis, G. C. Katsimiga, G. M. Koutentakis, and P. Schmelcher, New J. Phys. **21**, 043032 (2019).

[41] K. Keiler, S. Krönke, and P. Schmelcher, New J. Phys. **20**, 033030 (2018).

[42] K. Keiler and P. Schmelcher, New J. Phys. **20**, 103042 (2018).

[43] J. Chen, J. M. Schurer, and P. Schmelcher, Phys. Rev. Lett. **121**, 043401 (2018).

[44] A. S. Dehkharghani, A. G. Volosniev, and N. T. Zinner, Phys. Rev. Lett. **121**, 080405 (2018).

[45] A. Camacho-Guardian, L. A. Peña Ardila, T. Pohl, and G. M. Bruun, Phys. Rev. Lett. **121**, 013401 (2018).

[46] A. Klein and M. Fleischhauer, Phys. Rev. A **71**, 033605 (2005).

[47] S. I. Mistakidis, G. M. Koutentakis, G. C. Katsimiga, T. Busch, and P. Schmelcher, New J. Phys. **22**, 043007 (2020).

[48] J. Sous, M. Berciu, and R. V. Krems, Phys. Rev. A **96**, 063619 (2017).

[49] E. Compagno, G. De Chiara, D. G. Angelakis, and G. M. Palma, Sci. Rep. **7**, 2355 (2017).

[50] C. Charalambous, M. A. García-March, G. Muñoz-Gil, P. R. Grzybowski, and M. Lewenstein, Quantum **4**, 232 (2020).

[51] A. Boudjemâa, N. Guebli, M. Sekmane, and S. Khlifa-Karfa, J. Phys.: Condens. Matter **32**, 415401 (2020).

[52] S. A. Trugman, Phys. Rev. B **37**, 1597 (1988).

[53] C. L. Kane, P. A. Lee, and N. Read, Phys. Rev. B **39**, 6880 (1989).

[54] J. Koepsell, J. Vijayan, P. Sompet, F. Grusdt, T. A. Hilker, E. Demler, G. Salomon, I. Bloch, and C. Gross, Nature (London) **572**, 358 (2019).

[55] S. Sachdev, Phys. Rev. B **39**, 12232 (1989).

[56] J. Levinsen, M. M. Parish, and G. M. Bruun, Phys. Rev. Lett. **115**, 125302 (2015).

[57] R. S. Christensen, J. Levinsen, and G. M. Bruun, Phys. Rev. Lett. **115**, 160401 (2015).

[58] J. Jager, R. Barnett, M. Will, and M. Fleischhauer, Phys. Rev. Research **2**, 033142 (2020).

[59] A. Bohrdt, Y. Wang, J. Koepsell, M. Kánasz-Nagy, E. Demler, and F. Grusdt, Phys. Rev. Lett. **126**, 026401 (2021).

[60] G. E. Astrakharchik and L. P. Pitaevskii, Phys. Rev. A **70**, 013608 (2004).

[61] F. M. Cucchietti and E. Timmermans, Phys. Rev. Lett. **96**, 210401 (2006).

[62] R. M. Kalas and D. Blume, Phys. Rev. A **73**, 043608 (2006).

[63] M. Bruderer, A. Klein, S. R. Clark, and D. Jaksch, Europhys. Lett. **82**, 30004 (2008).

[64] M. Bruderer, A. Klein, S. R. Clark, and D. Jaksch, Phys. Rev. A **76**, 011605(R) (2007).

[65] A. Privitera and W. Hofstetter, Phys. Rev. A **82**, 063614 (2010).

[66] W. Casteels, J. Tempere, and J. T. Devreese, Phys. Rev. A **86**, 043614 (2012).

[67] W. Casteels, J. Tempere, and J. T. Devreese, Phys. Rev. A **88**, 013613 (2013).

[68] B. Kain and H. Y. Ling, Phys. Rev. A **94**, 013621 (2016).

[69] W. Li, and S. Das Sarma, Phys. Rev. A **90**, 013618 (2014).

[70] Y. E. Shchadilova, R. Schmidt, F. Grusdt, and E. Demler, Phys. Rev. Lett. **117**, 113002 (2016).

[71] S. P. Rath and R. Schmidt, Phys. Rev. A **88**, 053632 (2013).

[72] X. Li, G. Bighin, E. Yakaboylu, and M. Lemeshko, Mol. Phys. **117**, 1981 (2019).

[73] B. Kain and H. Y. Ling, Phys. Rev. A **98**, 033610 (2018).

[74] F. Grusdt, R. Schmidt, Y. E. Shchadilova, and E. Demler, Phys. Rev. A **96**, 013607 (2017).

[75] R. Alhyder, X. Leyronas, and F. Chevy, Phys. Rev. A **102**, 033322 (2020).

[76] M. Taglieber, A.-C. Voigt, T. Aoki, T. W. Hänsch, and K. Dieckmann, Phys. Rev. Lett. **100**, 010401 (2008).

[77] C.-H. Wu, I. Santiago, J. W. Park, P. Ahmadi, and M. W. Zwierlein, Phys. Rev. A **84**, 011601(R) (2011).

[78] M. A. García-March, B. Juliá-Díaz, G. E. Astrakharchik, T. Busch, J. Boronat, and A. Polls, New J. Phys. **16**, 103004 (2014).

[79] F. Serwane, G. Zürn, T. Lompe, T. B. Ottenstein, A. N. Wenz, and S. Jochim, Science **332**, 336 (2011).

[80] See Supplemental Material at http://link.aps.org/supplemental/10.1103/PhysRevA.104.L031301. for the description of (1) the MLMCTDHX method (2) the impurity correlations and densities, (3) the predictions of the mean-field ansatz, (4) the properties of heavy impurities and the effect of larger baths, and (5) homogeneous settings.

[81] S. I. Mistakidis, G. C. Katsimiga, P. G. Kevrekidis, and P. Schmelcher, New J. Phys. **20**, 043052 (2018).

[82] J. Erdmann, S. I. Mistakidis, and P. Schmelcher, Phys. Rev. A **98**, 053614 (2018).

[83] J. Erdmann, S. I. Mistakidis, and P. Schmelcher, Phys. Rev. A **99**, 013605 (2019).

[84] R. Roy, A. Gammal, M. C. Tsatsos, B. Chatterjee, B. Chakrabarti, and A. U. J. Lode, Phys. Rev. A **97**, 043625 (2018).

[85] B. Chatterjee, M. C. Tsatsos, and A. U. J. Lode, New J. Phys. **21**, 033030 (2019).

[86] P. Siegl, S. I. Mistakidis, and P. Schmelcher, Phys. Rev. A **97**, 053626 (2018).

[87] R. Horodecki, P. Horodecki, M. Horodecki, and K. Horodecki, Rev. Mod. Phys. **81**, 865 (2009).

[88] P. A. M. Dirac, Proc. Cambridge Philos. Soc. **26**, 376 (1930).

[89] J. Frenkel, *Wave Mechanics; Advanced General Theory* (Clarendon, Oxford, 1934).

[90] A. Raab, Chem. Phys. Lett. **319**, 674 (2000).

[91] L. Cao, I. Brouzos, S. Zöllner, and P. Schmelcher, New J. Phys. **13**, 033032 (2011).

[92] L. Cao, I. Brouzos, B. Chatterjee, and P. Schmelcher, New J. Phys. **14**, 093011 (2012).

[93] H.-D. Meyer, F. Gatti, and G. A. Worth, *Multidimensional Quantum Dynamics: MCTDH Theory and Applications* (Wiley-VCH, Weinheim, 2009).

[94] F. Köhler, K. Keiler, S. I. Mistakidis, H.-D. Meyer, and P. Schmelcher, J. Chem. Phys. **151**, 054108 (2019).

[95] K. Keiler and P. Schmelcher, Phys. Rev. A **100**, 043616 (2019).

[96] F. Theel, K. Keiler, S. I. Mistakidis, and P. Schmelcher, New J. Phys. **22**, 023027 (2020).

[97] K. Henderson, C. Ryu, C. MacCormick, and M. G. Boshier, New J. Phys. **11**, 043030 (2009).

[98] R. Grimm, M. Weidemüller, and Y. B. Ovchinnikov, Adv. At. Mol. Opt. Phys. **42**, 95 (2000).

[99] M. Olshanii, Phys. Rev. Lett. **81**, 938 (1998).

[100] M. Egorov, B. Opanchuk, P. Drummond, B. V. Hall, P. Hannaford, and A. I. Sidorov, Phys. Rev. A **87**, 053614 (2013).

[101] A. Álvarez, J. Cuevas, F. R. Romero, C. Hamner, J. J. Chang, P. Engels, P. G. Kevrekidis, and D. J. Frantzeskakis, J. Phys. B **46**, 065302 (2013).

[102] S. Krönke, L. Cao, O. Vendrell, and P. Schmelcher, New J. Phys. **15**, 063018 (2013).

[103] L. Cao, S. Krönke, O. Vendrell, and P. Schmelcher, J. Chem. Phys. **139**, 134103 (2013).

[104] L. Cao, V. Bolsinger, S. I. Mistakidis, G. Koutentakis, S. Krönke, J. M. Schurer, and P. Schmelcher, J. Chem. Phys. **147**, 044106 (2017).

[105] A. Amico, F. Scazza, G. Valtolina, P. E. S. Tavares, W. Ketterle, M. Inguscio, G. Roati, and M. Zaccanti, Phys. Rev. Lett. **121**, 253602 (2018).

[106] S. I. Mistakidis, G. C. Katsimiga, G. M. Koutentakis, T. Busch, and P. Schmelcher, Phys. Rev. Research **2**, 033380 (2020).

[107] S. I. Mistakidis, G. C. Katsimiga, G. M. Koutentakis, T. Busch, and P. Schmelcher, Phys. Rev. Lett. **122**, 183001 (2019).

[108] A. Bergschneider, V. M. Klinkhamer, J. H. Becher, R. Klemt, G. Zürn, P. M. Preiss, and S. Jochim, Phys. Rev. A **97**, 063613 (2018).

[109] K. Keiler, S. I. Mistakidis, and P. Schmelcher, New J. Phys. **22**, 083003 (2020).

[110] M. Bruderer, A. Klein, S. R. Clark, and D. Jaksch, New J. Phys. **10**, 033015 (2008).